Intrinsic contributions to the planar Hall effect in Fe and $Fe_3Si$ films on GaAs substrates



2006 J. Phys.: Condens. Matter 18 2641

(http://iopscience.iop.org/0953-8984/18/9/004)

INSTITUTE OF PHYSICS PUBLISHING JOURNAL OF PHYSICS: CONDENSED MATTER

J. Phys.: Condens. Matter **18** (2006) 2641–2653 doi:10.1088/0953-8984/18/9/004

# Intrinsic contributions to the planar Hall effect in Fe and $Fe_3Si$ films on GaAs substrates

**K-J Friedland, M Bowen, J Herfort, H P Schönherr and K H Ploog**

Paul-Drude-Institute for Solid State Electronics, Hausvogteiplatz 5-7, 10117 Berlin, Germany

E-mail: kjf@pdi-berlin.de

Received 18 October 2005
Published 17 February 2006
Online at stacks.iop.org/JPhysCM/18/2641

**Abstract**

We show that the antisymmetric planar Hall effect in Fe and $Fe_3Si$ layers grown on GaAs(113)A substrates and the symmetric intrinsic planar Hall effect in $Fe_3Si$ on GaAs(001) are closely related to each other. These effects appear in conjunction with additional contributions to the anomalous Hall effect, which reflect the magnetic field-induced crystalline anisotropy upon atomic ordering of the crystal. In the context of recent theoretical studies based on the Berry phase and the spin chirality, we explain the behaviour of the planar Hall effect with a microscopic model that takes into account dynamic non-coplanar spin configurations. We analyse such non-coplanar spin configurations, which are in accordance with the symmetry of the investigated systems, and find a good correspondence with experimental results.

(Some figures in this article are in colour only in the electronic version)

## 1. Introduction

Magnetotransport phenomena in ferromagnetic layers with in-plane external magnetic fields, including the anisotropic magnetoresistance (AMR) [1] and its twin the planar Hall effect (PHE) [2–4], are widely used to study the magnetization and its reversal as a function of the external magnetic field. In contrast to other methods such as superconducting quantum interference device (SQUID) magnetometry, magnetotransport measurements provide information on the magnetic behaviour of small volumes such as low-dimensional structures and are therefore of importance for spintronics.

The anomalous Hall effect (AHE), with magnetic fields perpendicular to the ferromagnetic layers, probes spin-dependent electron states and scattering by spontaneous magnetization. Presently, the theoretical understanding of the AHE has progressed considerably in the framework of Berry phase effects caused by the electron motion along non-coplanar spin configurations in systems such as manganites [5], spin-frustrated pyrochlore molybdates [6], and (III, Mn)V compounds [7]. A theoretical relation between the AHE and the $k$-space

  

Berry phase of occupied Bloch states has also been proposed for conventional ferromagnets such as bcc Fe [8]. In addition, a chirality-driven anomalous Hall effect due to non-trivial spin configurations was already studied for ferromagnets in the weak coupling regime [9], as realized in conventional transition metal ferromagnets. Thus, these new concepts generally relate magnetotransport to spin texture and magnetic ordering. Yet there is only little understanding of such Berry phase and spin chirality effects with respect to the AMR and the PHE.

Conventionally, the PHE in ferromagnetic layers is understood as originating from AMR, i.e., from the difference in resistivities between $\rho_{\parallel}$ and $\rho_{\perp}$ for orientations of the current along and perpendicular to the in-plane magnetization **M**, respectively. This difference gives rise to off-diagonal components in the magnetoresistivity tensor $\rho_{xy}$, which is conventionally called the planar Hall effect. The AMR-related origin of the PHE contrasts the ordinary and anomalous Hall effects which result from separation of charge by the Lorentz force or spins by the spin–orbit interaction.

Up to second order of magnetization contributions in the magnetoresistivity tensor, $\rho_{xx}$ and $\rho_{xy}$ exhibit the following dependence on the angle between the current and the magnetization $\theta_{\mathrm{M}}$ upon rotating a single-domain magnetization in the plane of a ferromagnetic and isotropic thin film [10, 11]:

$$\rho_{xx} = \rho_{\perp} + (\rho_{\parallel} - \rho_{\perp}) \cos^2(\theta_{\mathrm{M}}), \tag{1a}$$

$$\rho_{xy} = \rho^{s}_{xy} \cos(\theta_{\mathrm{M}}) \sin(\theta_{\mathrm{M}}). \tag{1b}$$

Both $\rho_{xx}$ and $\rho_{xy}$ are symmetric with respect to the direction of the magnetization. Conventionally, the quantities $\rho_{\parallel} - \rho_{\perp}$ and $\rho^{s}_{xy}$ are ascribed to the AMR and the symmetric PHE, respectively. Recent experiments have revealed additional contributions to the PHE in ferromagnetic systems with reduced symmetry. An additional symmetric contribution to the PHE was observed for stoichiometric $Fe_3Si$ when grown on GaAs(001) substrates [12]. $Fe_3Si$ with the $D0_3$ crystal symmetry can be regarded as a Heusler alloy with non-equivalent Fe sites. For two of the Fe sites, the nearest-neighbour environment is reduced to a tetragonal one. It was then argued [12] that different configurations of coherent spin fluctuations between the Fe sublattices are responsible for the additional PHE. Fe and $Fe_3Si$ layers grown on GaAs(113)A exhibit an antisymmetric contribution to the PHE [13–15] with respect to the direction of the magnetization. This reflects the so-called 'Umkehr' effect [16] when even and odd terms coexist in the off-diagonal components of the magnetoresistivity tensor due to crystal symmetry.

In this paper, we summarize experimental results that indicate that the antisymmetric PHE in Fe and $Fe_3Si$ layers grown on GaAs(113)A and the symmetric PHE in $Fe_3Si$ layers grown on GaAs(001)PHE are closely linked to the AHE. We systematically observe a sign change and large values of the PHE upon lowering the temperature when approaching the atomically well-ordered crystalline structure. As such we designate this PHE as intrinsic (IPHE) to the crystal lattice and its intersublattice interactions. In the context of recent studies of the Berry phase and spin chirality effects, we propose a microscopic model that takes into account dynamic non-coplanar spin configurations and that may explain the behaviour of the IPHE in (113)A oriented films. Our model relies only on symmetry arguments with respect to particular spin states as a result of intersublattice interactions for a given magnetic field-induced anisotropy.

## 2. Experimental details

Fe and $Fe_3Si$ layers with thicknesses between 9 and 89 nm were grown in an As-free molecular beam epitaxy (MBE) chamber connected to a III–V semiconductor MBE chamber via an

interlock. The growth of the GaAs buffer layers was performed on semi-insulating GaAs(001) and GaAs(113)A substrates at properly optimized conditions before transferring the samples through ultrahigh vacuum ($<1 \times 10^{-10}$ Torr) for subsequent Fe and $Fe_3Si$ growth. The growth temperature was 50 and 0 °C for Fe films on GaAs(001) and GaAs(113)A, respectively, and 250 °C for $Fe_3Si$. More details about the growth as well as the structural and morphological properties of the films can be found in [17, 18] for Fe and [19, 20] for $Fe_3Si$.

Magnetotransport measurements were carried out at stabilized temperatures. A programmable stepper motor was used to rotate the sample relative to the magnetic field direction. In most cases, we used Hall bar structures prepared by standard lithography techniques. The structures were carefully aligned to create a current flow along the $[33\bar{2}]$ and $[\bar{1}10]$ directions for films on GaAs(113)A substrates and along the $[\bar{1}10]$ and [110] directions for films on GaAs(001) substrates. These directions are all in-plane hard axes of magnetization, as a dominant fourfold magnetic anisotropy is observed in all investigated samples [19–21]. Ohmic contacts were obtained by bonding Au wires directly onto the Hall bar terminals, which results in sufficiently low contact resistances. In some cases, we used rectangular samples with an approximate size of $3 \times 4$ mm$^2$, for which we carefully aligned the terminals to achieve uniform current and equal potential lines at zero magnetic field. Nevertheless, because of the small transverse (planar Hall) resistivity $\rho_{xy}$ compared to the longitudinal resistivity $\rho_{xx}$, a crossover from $\rho_{xx}$ to $\rho_{xy}$ may occur due to non-perfect alignment of the Hall terminals as the field strength $H$ or the angle $\theta_H$ between the current and the external magnetic field is changed. We therefore corrected $\rho_{xy}$ to $\rho_{xy}^{\mathrm{corr}}(H, \theta_H) = \rho_{xy}(H, \theta_H) - t\rho_{xx}(H, \theta_H)$, while keeping the weight $t$ fixed for all measurements of a particular contact configuration at a fixed temperature. Here $t$ is of the order $1\text{–}10 \times 10^{-5}$. No significant differences in the magnetoresistivities as a function of the magnetic field strength were found for lithographically processed Hall bar structures and rectangular samples. To measure the transverse magnetoresistance, we chose a contact configuration that results in a negative Hall voltage for an n-type semiconductor sample in the conventional Hall geometry. We define the corresponding magnetic field direction as being positive.

## 3. Results and discussion

### *3.1. Intrinsic PHE in Fe and $Fe_3Si$ grown on GaAs(113)A and GaAs(001) substrates*

An unusual Hall effect was observed in Fe and $Fe_{3+x}Si_{1-x}$ layers grown on GaAs(113)A substrates. This is a saturated antisymmetric planar Hall effect (SAPHE), $\rho_{xy}^{\mathrm{SAPHE}}$, which reflects a transverse electric field, when the magnetic field is aligned along the $[33\bar{2}]$ direction [13–15], and which can be regarded as manifestation of the 'Umkehr effect' [16] due to the crystal symmetry. The SAPHE exists even for a current that is aligned along the same $[33\bar{2}]$ direction, i.e., even when the current and magnetic field are parallel. In the following we briefly summarize the previous major experimental results on which the unified model relies. We present in figure 1(a) the magnetic field dependences of $\rho_{xy}$ at $T = 300$ K for a 10 nm thick Fe film grown on a GaAs(113)A substrate. For magnetic fields above $H_{\mathrm{sat}} \approx 0.2$ kOe, $\rho_{xy}$ becomes completely saturated. Upon sweeping the magnetic field to the opposite direction, $\rho_{xy}$ changes sign, which is never observed for Fe and $Fe_3Si$ layers grown on GaAs(001) [14, 15].

To prove the real antisymmetry of the transverse magnetoresistivity with respect to Onsager's relation $\rho_{xy}(\boldsymbol{\alpha}) = \rho_{yx}(-\boldsymbol{\alpha})$, where the vector $\boldsymbol{\alpha}$ represents the direction of the magnetization, we measured $\rho_{xy}$ and $\rho_{yx}$ by interchanging the current and voltage terminals and examined the symmetric $(\rho_{xy} + \rho_{yx})/2$ and antisymmetric $(\rho_{xy} - \rho_{yx})/2$ contributions to the planar Hall effect (see figures 1(a) and (b)). This analysis reveals the antisymmetry, which

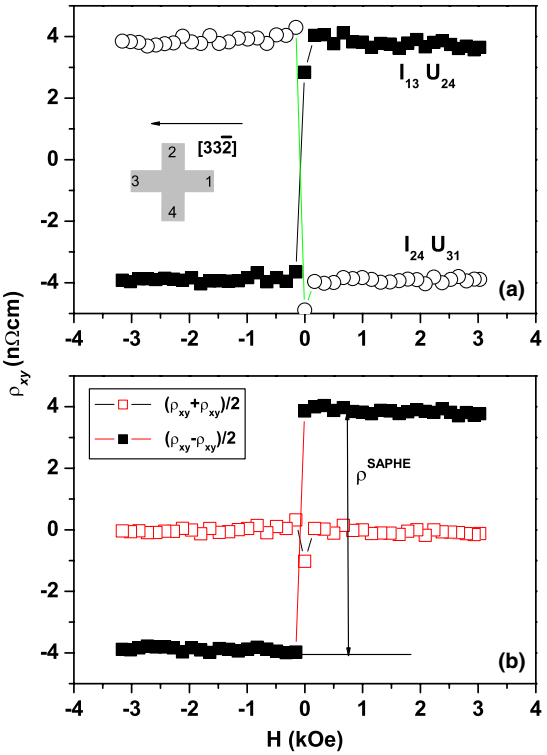


**Figure 1.** (a) Planar Hall effect response at $T = 300$ K of a 10 nm thick Fe film grown on GaAs(113)A for a magnetic field applied along [33$\bar{2}$]. The inset depicts the sample and contact geometry. (b) The separation of the symmetric and antisymmetric contributions to the PHE data of panel (a).

is defined as $\rho_{xy}^{\mathrm{SAPHE}} = \rho_{xy}^{a}(H > +H_{\mathrm{sat}}) - \rho_{xy}^{a}(H < -H_{\mathrm{sat}})$. No $\rho_{xy}^{\mathrm{SAPHE}}$ was observed for magnetic fields along the [$\bar{1}$10] direction. A similar $\rho_{xy}^{\mathrm{SAPHE}}$ was found in $Fe_{3+x}Si_{1-x}$ layers grown on GaAs(113) substrates [13]. It is important to note that the observed $\rho_{xy}^{\mathrm{SAPHE}}$ does not arise from an AHE component due to a slight but unavoidable out-of-plane sample misalignment, since such a contribution from the AHE would appear as a slope in the high-field region. Furthermore, the antisymmetry of $\rho_{xy}^{\mathrm{SAPHE}}$ is clearly in contrast to other phenomena such as the 'giant planar Hall effect' in (Ga, Mn)As [3], for which an apparent antisymmetry arises from carrier scattering at domain walls and which can in fact be attributed to a symmetric PHE.

In the case of thin films grown epitaxially on GaAs(113)A substrates, rotating the magnetic field in the film plane leads to a rotation of the magnetization in the low-symmetry (113) plane of the crystal lattice. As a consequence, we no longer observe a four-fold symmetry in $\rho_{xy}$, as evidenced in figure 2 by the dependence of $\rho_{xy}$ on $\theta_{\mathrm{M}}$ for a $Fe_{3+x}Si_{1-x}$ layer near the $Fe_3Si$ stoichiometric composition with $x = 0.07$ at (a) $T = 300$ K and (b) $T = 77$ K. Here $\theta_{\mathrm{M}}$ is the angle between the direction of magnetization and the current direction along the [33$\bar{2}$] axis.

We calculate $\theta_{\mathrm{M}}$ from the $\rho_{xx}$ data using (1*a*) as described in [14]. This symmetry reduction in the transport related magnetocrystalline anisotropy is not supported by SQUID magnetization measurements, which are in accordance with a four-fold magnetocrystalline anisotropy [20]. Recently, we have shown how $\rho_{xy}^{\mathrm{SAPHE}}$ is phenomenologically related to a third-order contribution of the magnetoresistivity tensor. For the classical crystal class $m3m$, to

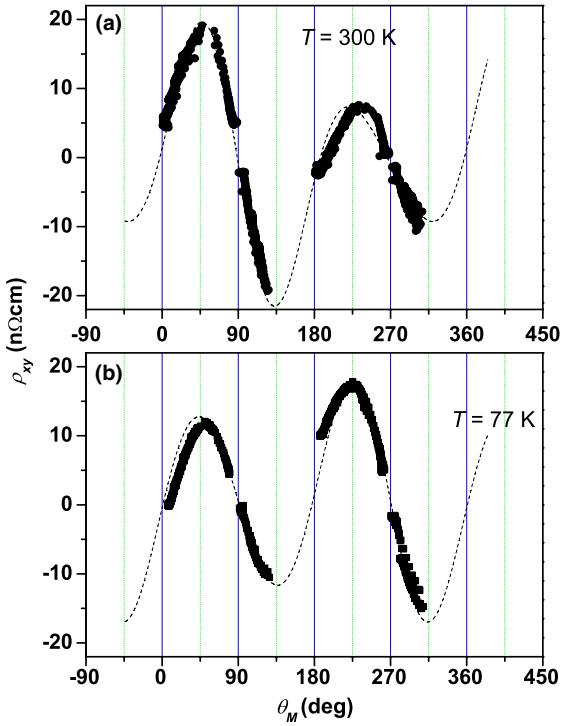


**Figure 2.** Planar Hall effect response of a 40 nm thick $Fe_{3+x}Si_{1-x}$ ($x = 0.07$) film grown on GaAs(113)A with a current along $[33\bar{2}]$ as a function of the angle $\theta_M$ between magnetization and current at saturated magnetic field and at (a) $T = 300$ K, (b) $T = 77$ K. The dotted lines are fits to (2) with $\rho_{xy}^{s(113)} = 40$ nΩ cm, $\rho_{xy}^{\mathrm{SAPHE}} = 3.6$ nΩ cm at $T = 300$ K and $\rho_{xy}^{s(113)} = 36$ nΩ cm, $\rho_{xy}^{\mathrm{SAPHE}} = -1.2$ nΩ cm at $T = 77$ K.

which both $Fe_3Si$ ($Fm3m$) and Fe ($Im3m$) belong, one can find for $\rho_{xy}^{(113)}$, which corresponds to a current applied along $[33\bar{2}]$ and a voltage measured along $[\bar{1}10]$, an expression valid up to the third order of magnetization [15]:

$$\rho_{xy}^{(113)} = \rho_{xy}^{s(113)} \sin(\theta_M)\cos(\theta_M) + \rho_{xy}^{a(113)}[(33/5)\cos(\theta_M) - (84/15)\cos^3(\theta_M)]. \quad (2)$$

In addition to the conventional symmetric second-order contribution $\rho_{xy}^{s(113)} \sin(\theta_M)\cos(\theta_M)$, $\rho_{xy}^{(113)}$ exhibits an additional antisymmetric term of third order with an amplitude of $\rho_{xy}^{a(113)}$. This term can directly be related to $\rho_{xy}^{\mathrm{SAPHE}}$. This result is qualitatively different from the PHE observed for GaAs(001) substrates which, given the symmetry conditions of this phenomenological approach, can only contain even-order terms. (2) is in line with the experimental observation on (113)A-oriented films of an additional contribution to the planar Hall effect (second term in (2)) that changes sign upon reversing the direction of the magnetic field. This antisymmetric term is also called the second-order Hall effect.

It is an interesting novel result of the present sample that $\rho_{xy}^{\mathrm{SAPHE}}$ changes sign with decreasing temperature from $T = 300$ K down to $T = 77$ K, which manifests itself in figures 2(a) and (b) as an interchange of the maximum values at $\theta_M = 45°$ and 225°, respectively. However, the AMR signal ($\rho_\perp - \rho_\parallel$) does not change its sign. In addition, we do not observe a sign change of $\rho_{xy}^{\mathrm{SAPHE}}$ with temperature for $Fe_{3+x}Si_{1-x}$ films away from the $Fe_3Si$ stoichiometric composition with $|x| > 0.1$. The sign of $\rho_{xy}^{\mathrm{SAPHE}}$ is negative for layers

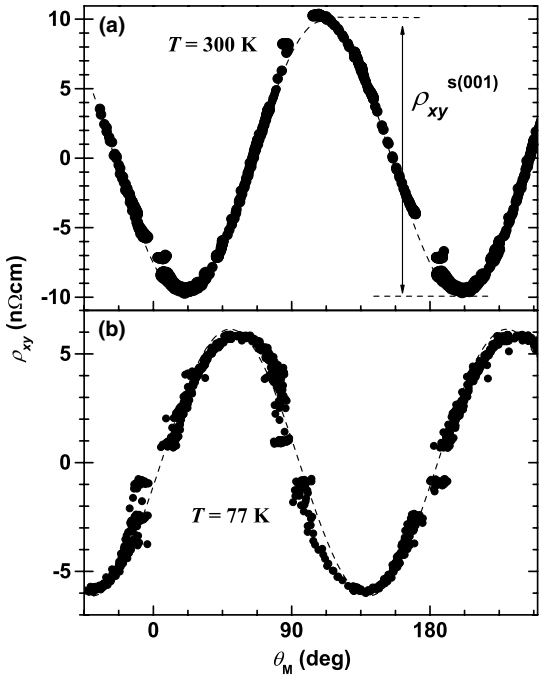


**Figure 3.** Planar Hall effect response of a 40 nm thick $Fe_{3+x}Si_{1-x}$ ($x = 0.01$) film grown on GaAs(001) with a current along [$\bar{1}$10] as a function of the angle $\theta_M$ between magnetization and current at saturated magnetic field and at (a) $T = 300$ K, (b) $T = 77$ K. The dotted lines are fits to (1*b*) with $\rho_{xy}^{s(001)} = 19$ n$\Omega$ cm, at $T = 300$ K and $\rho_{xy}^{s(001)} = -12$ n$\Omega$ cm at $T = 77$ K.

near the $Fe_3Si$ stoichiometric composition at low temperatures and of the same sign as the one for Fe layers on GaAs(113)A substrates, even though the sign of $\rho_\perp - \rho_\parallel$ is opposite in Fe and $Fe_{3+x}Si_{1-x}$ layers.

$Fe_{3+x}Si_{1-x}$ layers grown on GaAs(001) show a symmetric PHE with an amplitude $\rho_{xy}^{s(001)}$ according to (1*b*). Compared to $\rho_{xy}^{\mathrm{SAPHE}}$, $\rho_{xy}^{s(001)}$ also changes sign upon lowering the temperature from $T = 300$ to 77 K in nearly stoichiometric $Fe_3Si$ grown on GaAs(001) [12]. Figures 3(a) and (b) present the dependences of $\rho_{xy}$ on $\theta_M$ at (a) $T = 300$ K and (b) at $T = 77$ K for a (001)-oriented sample with $x = +0.01$ with a current along [110].

We interpret the sign change as resulting from an additional symmetric IPHE contribution $\rho_{xy}^{\mathrm{symmIPHE}}$ of opposite sign that is present in addition to the conventional AMR term $\rho_{xy}^{\mathrm{AMR}} = \rho_\parallel - \rho_\perp$ [12].

$\rho_{xy}^{\mathrm{symmIPHE}}$ is negative and in fact represents the anisotropic contribution to the PHE due to crystalline symmetry. With decreasing temperature, $|\rho_{xy}^{\mathrm{symmIPHE}}|$ increases and eventually compensates $\rho_{xy}^{\mathrm{AMR}}$ at $T_{\mathrm{ord}}$. We note that $T_{\mathrm{ord}}$ reaches the maximum value of $T_{\mathrm{ord}}^{\mathrm{max}} \approx 251$ K for a nearly stoichiometric sample ($x = +0.01$). In contrast to this behaviour, non-stoichiometric $Fe_{3+x}Si_{1-x}$ layers with $|x| > 0.1$ show no sign change in the PHE down to $T = 4.2$ K.

### *3.2. Composition and temperature dependence of the symmetric and antisymmetric PHE in $Fe_3Si$*

We have previously shown that a significant degree of atomic ordering of the $Fe_{3+x}Si_{1-x}$ crystals occurs around $|x| < 0.1$ [12, 22, 23]. In this case, the sheet resistivity $\rho_{xx}$ exhibits

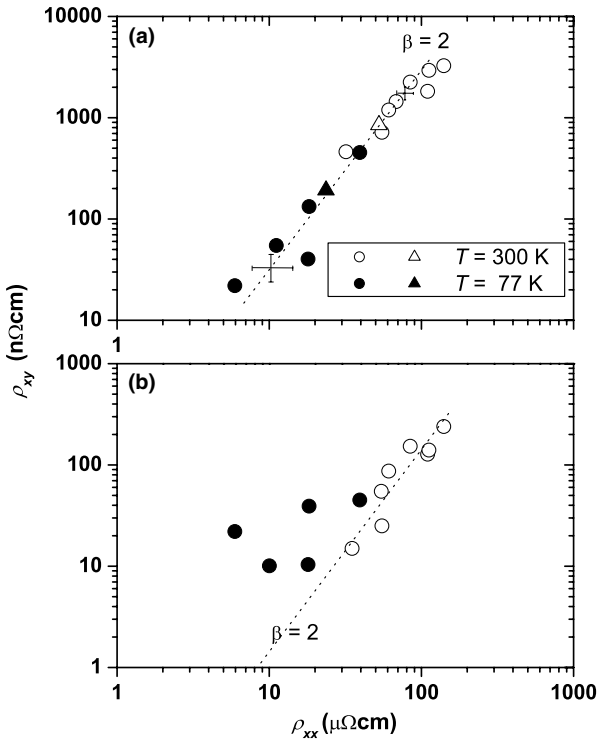


**Figure 4.** (a) Anomalous Hall effect and (b) planar Hall effect in $Fe_{3+x}Si_{1-x}$ films as a function of the resistivity. The dotted lines represent the power law $\rho_{xy} \propto \rho_{xx}^{\beta}$ with $\beta = 2$, $T = 300$ K. A common legend describes both panels: circles and triangles for (001) and (113)A substrates, respectively.

a deep minimum around $x = 0$, while the conductivity ratio $\rho^{300\ \mathrm{K}}/\rho^{77\ \mathrm{K}}$ for resistivities $\rho_{xx}$ at $T = 300$ and 77 K increases to a value of five, indicating the suppression of alloy scattering and the dominance of phonon scattering at high temperatures at nearly stoichiometric composition.

At the same time, ordered $Fe_3Si$ layers grown on GaAs(001) and GaAs(113)A substrates respectively give rise at low temperature to additional, negative contributions $\rho_{xy}^{\mathrm{symmIPHE}}$ and $\rho_{xy}^{\mathrm{SAPHE}}$ to the planar Hall effect (PHE), which we therefore ascribe as intrinsic to a more ordered $Fe_3Si$ Heusler alloy lattice. To find the relationship of different contributions in the PHE, we examine the composition and temperature dependences of $\rho_{xy}^{\mathrm{SAPHE}}$ and $\rho_{xy}^{s(001)}$ as compared to the anomalous Hall effect $\rho_{xy}^{\mathrm{AHE}}$ measured in the conventional Hall geometry with the magnetic field perpendicular to the film plane.

Figure 4(a) shows the anomalous Hall effect in $\rho_{xy}^{\mathrm{AHE}}$ for $Fe_{3+x}Si_{1-x}$/GaAs(001) layers as a function of sheet resistivity $\rho_{xx}$. Changes to $\rho_{xx}$ encompass varying the measurement temperature either to $T = 77$ or 300 K, film thickness between 9 and 87 nm, as well as composition $x$. We find a general scaling dependence $\rho_{xy}^{\mathrm{AHE}} \propto \rho_{xx}^{\beta}$ with $\beta \cong 2$, similar to the one found for Fe layers grown on GaAs [13]. This scaling spans over ordered and disordered samples for both high and low temperatures, indicating that the physical origin of $\rho_{xy}^{\mathrm{AHE}}$ does not depend on whether the scattering is related to phonons or impurities. A scaling with $\beta = 2$ is ascribed to an extrinsic side-jump scattering [24] or to intrinsic scattering processes [25]. As shown in figure 4(b), the same scaling behaviour with $\beta \cong 2$ is also found for the symmetric planar Hall effect $\rho_{xy}^{s(001)} \propto \rho_{xx}^{\beta}$ in disordered $Fe_{3+x}Si_{1-x}$ samples with $x > 0.1$ or in ordered

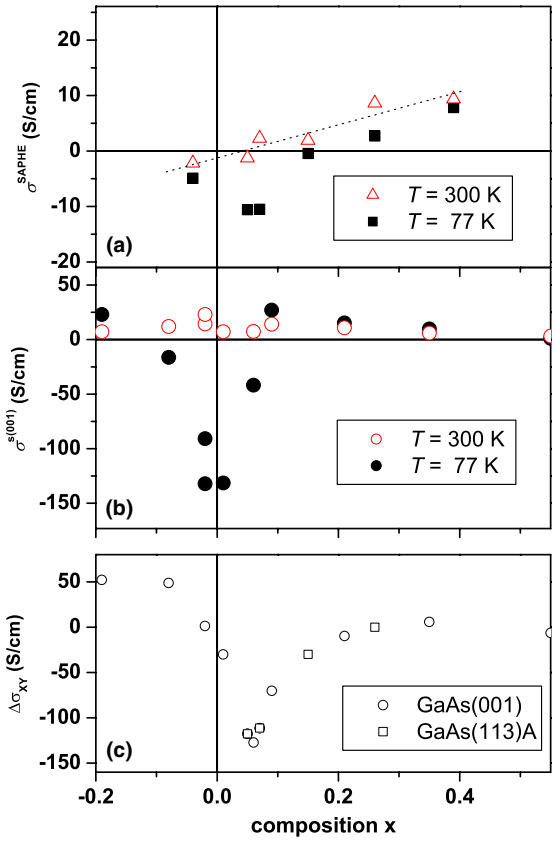


**Figure 5.** The saturated antisymmetric PHE, (b) the symmetric planar Hall effect and (c) the anomalous Hall effect in $Fe_{3+x}Si_{1-x}$ films as a function of composition $x$ for $T = 300$ and $T = 77$ K.

samples at high temperatures. In contrast, $\rho_{xy}^{s(001)}$ in well-ordered samples at low temperatures is significantly larger than one would expect from the extrapolated scaling dependence $\rho_{xy}^{s(001)} \propto \rho_{xx}^2$ (i.e., for low $\rho_{xx}$). This reflects the additional contribution $\rho_{xy}^{\text{symmIPHE}}$ in this case and indicates a different physical origin of $\rho_{xy}^{\text{symmIPHE}}$ as compared to the conventional symmetric planar Hall effect in disordered samples or at high temperatures. Unfortunately, a similar analysis is not possible for the present set of $Fe_{3+x}Si_{1-x}$/GaAs (113)A samples due to a much too narrow range of resistivities. Therefore, we calculate the corresponding Hall conductivities $\sigma^{s(001)}$, $\sigma^{\text{SAPHE}}$ and $\sigma^{\text{AHE}}$ according to $\sigma = \rho_{xy}/\rho_{xx}^2$ in order to demonstrate the relationship between these quantities around $x = 0$.

We present in figures 5(a) and (b) the compositional dependences of the SAPHE and the symmetrical PHE at $T = 300$ and 77 K. At high temperatures, $\sigma^{\text{SAPHE}}$ and $\sigma^{s(001)}$ vary slowly with $x$, which one could expect from the $\rho_{xy}^{s(001)} \propto \rho_{xx}^2$ scaling [see figure 4(b)]. However, at low temperatures, $\sigma^{\text{SAPHE}}$ and $\sigma^{s(001)}$ change rapidly with a minimum around $x = 0$. In addition, figure 5(c) shows the compositional dependence of the AHE conductivity difference $\Delta\sigma^{\text{AHE}} = \sigma_{\text{min}}^{\text{AHE}} - \sigma^{\text{AHE}}(300\text{ K})$ between the value found at $T = 300$ K and the minimum value $\sigma_{\text{min}}^{\text{AHE}}$ (for most of the samples $\sigma^{\text{AHE}}$ decreases by lowering the temperature to a minimum value around $T = 100$ K (not shown here); the temperature dependence of $\sigma^{\text{AHE}}$ will be discussed elsewhere). We thus observe a minimum near $x = 0$. From the phenomenological

point of view, the negative contributions in $\sigma^{\mathrm{SAPHE}}$ and $\sigma^{s(001)}$ are higher-order contributions in the magnetoresistivity tensor in the presence of the magnetic field and due to crystalline anisotropy with ordering of the crystal that are third-order contributions for $Fe_{3+x}Si_{1-x}$/GaAs (113)A (see (2)) and fourth-order contributions for $Fe_{3+x}Si_{1-x}$/GaAs (001). For the case of $Fe_{3+x}Si_{1-x}$/GaAs (113)A, it was shown that these higher-order contributions also appear in the AHE [15] and may result in a negative $\Delta\sigma^{\mathrm{AHE}}$ around $x = 0$.

## 4. Discussion of the PHE for nearly stoichiometric $Fe_3Si$

Note that in nearly stoichiometric $Fe_3Si$ the absolute values of $\sigma^{\mathrm{SAPHE}}$, $\sigma^{s(001)}$ and $\Delta\sigma^{\mathrm{AHE}}$ are large and reach more than 100 S $m^{-1}$. Recently, large anomalous Hall conductivities were attributed to Berry phase effects. It was shown by experimental and theoretical studies that a finite AHE may exist in systems with more than two non-coplanar spin sublattices [26, 27]. An anomalous Hall effect contribution that is related to the $k$-space Berry phase of occupied Bloch states was even predicted for ferromagnetic bcc Fe [8]. According to this explanation, the AHE arises due to the conduction of carriers from a very narrow portion of the Fermi surface that is split by the spin–orbit interaction. The near degeneracy of spin-up and spin-down states at such points in the band structure may thus give rise to a non-trivial spin topology throughout the ferromagnet's lattice. The anomalous Hall conductivity will then be proportional to this Berry phase and results in large anomalous Hall conductivities, as observed in the AHE and the IPHE in Fe and $Fe_3Si$ layers.

Fe and $Fe_3Si$ are systems with a clear band magnetism [28]; therefore, static non-coplanar spin configurations like the ones in frustrated spin systems do not exist. Nevertheless, non-coplanar spin configurations may arise statically around defects or dynamically due to spin fluctuations, spin waves, and magnons [29]. As a result, carriers are moving in a magnetic field that varies in space and time due to the background of fluctuating local moments. As a result, a Berry phase arises that contributes to the conductivity. Due to the high symmetry of $Fe_3Si$, multiply degenerate contributions to the AHE or PHE from the ensemble of possible spin configurations will cancel out, while the Berry phase remains intact. Extended theoretical calculations of the band structure are needed in order to find out which parts in $k$-space of $Fe_3Si$ may result in an intrinsic AHE and therefore also in the IPHE.

The strong temperature dependence of the IPHE, and the good agreement between $T_{\mathrm{ord}}$ and the exchange energy $J_{\mathrm{ex}}[(\mathrm{B} \leftrightarrow (\mathrm{A}, \mathrm{C})] = 145$ K between the $Fe_3Si$ B and (A, C) sublattices calculated by Stearns [28] from Mössbauer spectroscopy on a $Fe_3Si$ powder, led us to propose a microscopic description for the appearance of $\rho_{xy}^{\mathrm{symmIPHE}}$ [12]. This model considers spin interactions between the non-equivalent sublattices in the $Fe_3Si$ Heusler alloy. Coherent spin fluctuations between sublattices resulting from such interactions were argued to give rise to the formation of non-coplanar spin configurations.

Tatara *et al* [9] studied theoretically the relationship between the anomalous Hall effect and non-trivial spin configurations in ferromagnets in the weak coupling regime, which is the case for all transition metal ferromagnets including Fe and $Fe_3Si$. The interaction of the carrier spins with the slowly varying background of localized spins $S_X$ leads to an anomalous Hall conductivity

$$\sigma_{xy}^{(3)} = (4\pi)^2 \sigma_0 J^3 \nu^2 \tau \chi_0, \tag{3}$$

where $\chi_0 = \frac{1}{6N} \sum_{\boldsymbol{X}_i} S_{\boldsymbol{X}_1} \cdot (S_{\boldsymbol{X}_2} \times S_{\boldsymbol{X}_3})[f(\boldsymbol{X}_1, \boldsymbol{X}_2, \boldsymbol{X}_3)]$ is the uniform (or net) chirality, $\sigma_0$ is the Drude conductivity, $J$ the exchange coupling coefficient, $\tau$ the scattering time and $\nu$ is the density of states. $f(\boldsymbol{X}_1, \boldsymbol{X}_2, \boldsymbol{X}_3)$ is a numerical factor that depends on the spatial position of the different spins. This Hall contribution is of second order and encompasses also a third-order

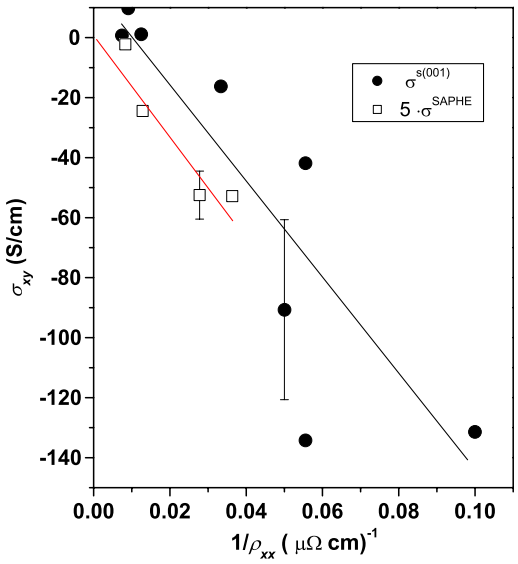


**Figure 6.** Dependence of the conductivities $\sigma^{s(001)}$ and $\sigma^{\mathrm{SAPHE}}$ on the inverse film resistivity $1/\rho_{xx}$ for different composition at $T = 77$ K for $Fe_{3+x}Si_{1-x}$ on GaAs(001) and GaAs(113)A substrates. The error bars correspond to statistical variation in the $\rho_{xy}^{s(001)} \propto \rho_{xx}^2$ law in figure 4(a).

term with respect to the exchange interaction. It is dominant in the clean, well-ordered regime and at low temperatures, as it is the case here near the $Fe_3Si$ stoichiometric composition.

We have already shown [15], that at least the $\rho^{\mathrm{SAPHE}}$ for the (331)A case is a second-order Hall effect

$$\rho^{\mathrm{SAPHE}} = \rho_{xy}^{a(113)} = 9(a_{32221} + a_{31121} - 2a_{33321})/(22\sqrt{2}), \tag{4}$$

which phenomenologically is described by the third-order components $a_{32221}$, $a_{31121}$ and $a_{33321}$ in the magnetoresistivity tensor, expanded in ascending powers of magnetization. For the crystal class $m3m$, to which both $Fe_3Si$ ($Fm3m$) and Fe ($Im3m$) belong, $a_{32221}+a_{31121}-2a_{33321}$ simplifies to $2(a_{12223}-a_{11123})$ [30]. In fact the quantities $a_{ijklm}$ are the $i, j, k$ partial derivatives with respect to the magnetization directions of the $l, m$ components of the magnetoresistivity tensor, and reflect the longitudinal and transverse resistivities by a simultaneous change of three magnetization components along the $i, j, k$ directions. In addition, (4) shows that the magnetization components of all directions contribute to $\rho^{\mathrm{SAPHE}}$. For our microscopic model we reverse this conclusion by stressing that any non-coplanar spin or moment configuration with a non-zero chirality will contribute to higher-order contributions in the magnetoresistivity tensor. In $Fe_3Si$, for example, $a_{ijklm}$ would describe a coherent three-spin interaction between three non-equivalent Fe sites. However, the possible mechanisms to achieve a finite net chirality are still the subject of debate [31]. As discussed by Tatara [9], in regular lattices with simple nearest-neighbour exchange interactions, chiralities on adjacent plaquettes tend to cancel out each other due to symmetry.

The chirality-driven anomalous Hall conductivity described by (3) is proportional to the scattering time $\tau$, which implies a different mechanism for this AHE as compared to the resistivity $\rho_{xy}^{\mathrm{AHE}} \propto \rho_{xx}^2$ for the disordered case [see figure 4(a)]. The behaviour of $\sigma^{\mathrm{SAPHE}}$ and $\sigma^{s(001)}$ for $Fe_{3+x}Si_{1-x}$ around $x = 0$ and at low temperatures suggests that the IPHE can be described by an equation similar to (3) as the resistivity decreases significantly for atomically ordered samples. To demonstrate this hypothesis, we plot in the figure 6 $\sigma^{\mathrm{SAPHE}}$ and $\sigma^{s(001)}$

as a function of the inverse resistivity. This shows that the absolute value of both conductivities increases with $\tau$, although with a large scatter in the values, which should be expected, given that these data are extracted from samples with different composition.

Finally, in the context of (3), we use the spin chirality of on-site spins given the $Fe_3Si$ crystal symmetry to demonstrate qualitatively the sign change of the SAPHE with atomic ordering of the lattice. The unit cell of $Fe_3Si$ consists of four sublattices. The D sublattice consists of Si sites, while the other three labelled A, B, and C contain the magnetically non-equivalent Fe sites. The Fe on the A, C sublattices with only four nearest-neighbour Fe sites carry a magnetic moment of 1.06 $\mu_B$, while the Fe in the B sublattice with eight nearest-neighbour Fe sites carries a moment of 2.23 $\mu_B$.

We consider particular triads of spins $\mathbf{S}_A$, $\mathbf{S}_B$ and $\mathbf{S}_C$ on the A, B, C sites of the lattice with a dominant component along the macroscopic magnetization direction $\mathbf{m}$. Within the unit cell, an on-site spin $\mathbf{S}$ may deviate from $\mathbf{m}$, whereby the deviation $\boldsymbol{\Delta}\mathbf{S}$ orients along preferential directions due to an inner cell anisotropy of the spin density distribution (SDD). The SDD of $Fe_3Si$ has been inferred by Moss and Brown from neutron diffraction experiments [32]. The SDD for all Fe sites is extended along the $\langle 100\rangle$ directions, which define the easy axes of magnetization. In addition, the SDD around the Fe (A, C) sites exhibits lobes that point towards the Si D sites along the $\langle 111\rangle$ directions. We will use these directions in order to define preferential orientations of spin fluctuations $\boldsymbol{\Delta}\mathbf{S}_A$ and $\boldsymbol{\Delta}\mathbf{S}_C$ on the $Fe_3Si$ A and C sublattices in the ordered case. We will contrast this to the disordered case, which encompasses both structural and thermal disorder. Structurally, the substitution of Si on Fe sites leads to a chemical environment around A and C sites with a greater chemical symmetry than the tetragonal one in the ordered case. Thermally, the disruption of intersublattice exchange interactions also increases the symmetry of fluctuations on such sites. Thus, both forms of disorder lead to additional configurations of spin fluctuations. Regarding the B sublattice sites, the surrounding SDD is nearly isotropic, so that we assume that the spin fluctuation $\boldsymbol{\Delta}\mathbf{S}_B$ can rotate freely in accordance with the constriction that the magnetization $\mathbf{M} = 2\mathbf{S}_B + \mathbf{S}_A + \mathbf{S}_C$ oriented along $\mathbf{m}$.

We now show that the spin chirality $\chi = \mathbf{S}_B \cdot (\mathbf{S}_C \times \mathbf{S}_A)$ that determines the intrinsic magnetotransport may become non-zero for certain directions of the magnetization $\mathbf{M}$ and may become positive or negative in both the ordered and the disordered cases for a given $\mathbf{M}$. It is straightforward to show that $\chi = \mathbf{M} \cdot (\boldsymbol{\Delta}\mathbf{S}_C \times \boldsymbol{\Delta}\mathbf{S}_A)$ so that we may consider the influence of spin chirality directly on spin fluctuation triads (SFTs). As an example, we present in figure 7(a) the sketch in the disordered case of an SFT $\boldsymbol{\Delta}\mathbf{S}_A$, $\boldsymbol{\Delta}\mathbf{S}_B$, and $\boldsymbol{\Delta}\mathbf{S}_C$ for (113)A-oriented $Fe_3Si$ that is used to compose a magnetization $\mathbf{M}$ along $[33\bar{2}]$. $\boldsymbol{\Delta}\mathbf{S}_A$ and $\boldsymbol{\Delta}\mathbf{S}_C$ are oriented along $[1\bar{1}1]$ and $[\bar{1}11]$, respectively. Such an SFT yields a positive spin chirality. Upon reversing the direction of $\mathbf{M}$, this SFT may transform such that $\boldsymbol{\Delta}\mathbf{S}_A$ is along $[\bar{1}1\bar{1}]$ and $\boldsymbol{\Delta}\mathbf{S}_C$ is along $[1\bar{1}\bar{1}]$, leading to a sign change in $\chi$. We emphasize that, for this configuration, the spin fluctuation $\boldsymbol{\Delta}\mathbf{S}_A$ points towards a nearest-neighbour D site, while $\boldsymbol{\Delta}\mathbf{S}_C$ points towards a nearest-neighbour Fe site, i.e., describing the disordered case. As an example in the ordered case, figure 7(b) shows the sketch of an SFT for $\mathbf{M}$ along $[33\bar{2}]$ with $\boldsymbol{\Delta}\mathbf{S}_A$ along $[1\bar{1}1]$ and $\boldsymbol{\Delta}\mathbf{S}_C$ along $[1\bar{1}\bar{1}]$ that leads to $\chi < 0$, i.e., opposite to the one of the SFT in figure 7(a). This implies that the sign change in $\chi$ upon ordering could reflect the switching in one of the A or C on-site fluctuations from a B to a D site. Thus, this sketch can describe the SAPHE in (113)A-oriented well-ordered $Fe_3Si$ when intersublattice interactions control the orientations of spin fluctuations. In the case of the Fe lattice, no such temperature-induced sign change of $\chi$ can occur for a possible spin chirality-driven SAPHE in agreement with the constant sign of $\rho^{SAPHE}$ at low and high temperatures.

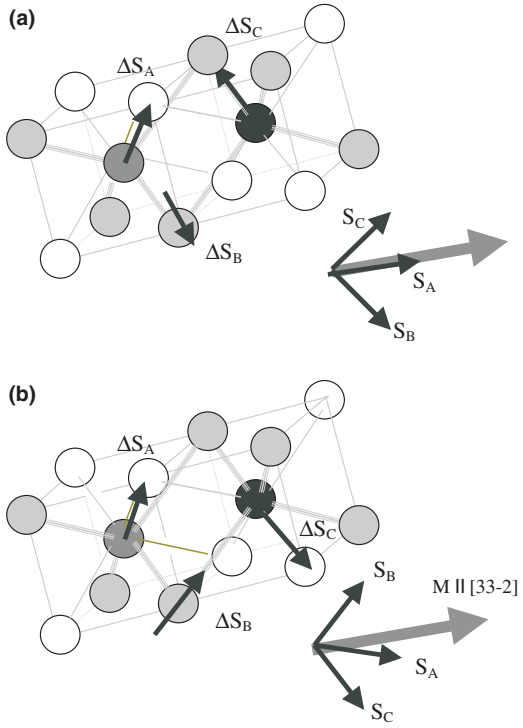


**Figure 7.** A spin fluctuation triad in (113)A-oriented $Fe_3Si$ with (a) $\mathbf{\Delta S}_A$ along $[1\bar{1}1]$ and $\mathbf{\Delta S}_C$ along $[\bar{1}11]$ describing the atomically disordered lattice and (b) $\Delta\mathbf{S}_A$ along $[1\bar{1}1]$ and $\mathbf{\Delta S}_C$ along $[1\bar{1}\bar{1}]$ describing the atomically ordered lattice. In both panels, the spin $\mathbf{S}_B$ can orient freely to form a triad corresponding to a magnetization along $[33\bar{2}]$.

## 5. Conclusion

The intrinsic planar Hall effect in ferromagnetic Fe and $Fe_3Si$ layers grown on GaAs(001) and GaAs(113)A substrates appears in conjunction with additional contributions to the anomalous Hall effect (AHE) and reflects the magnetic field-induced crystalline anisotropy upon atomic ordering of the crystal. We have shown that the IPHE follows a different scaling behaviour as compared to the disordered case. We describe this difference using a microscopic model that takes into account collective spin fluctuations and the non-trivial spin topology of the $Fe_3Si$ lattice given the symmetry of the investigated systems, and we find a good correlation between the results of the model and the experiment.

## Acknowledgments

We thank A Riedel for technical assistance and H Kostial, P K Muduli, P Kleinert, Y Takagaki and G Tatara for stimulating discussions.

## References

[1] McGuire T R and Potter R I 1975 *IEEE Trans. Magn.* **11** 1018
[2] Mitze C, Osthöver C, Voges F, Hasenkox U, Waser R and Arons R R 1999 *Solid State Commun.* **109** 189

[3] Tang H X, Kawakami R K, Awschalom D D and Roukes M L 2003 *Phys. Rev. Lett.* **90** 107201
[4] Friedland K-J, Kästner M and Däweritz L 2003 *J. Supercond.* **16** 261
[5] Lyanda-Geller Y, Chun S H, Salamon M B, Goldbart P M, Han P D, Tomioka Y, Asamitsu A and Tokura Y 2001 *Phys. Rev.* B **63** 184426
[6] Taguchi Y, Oohara Y, Yoshizawa H, Nagaosa N and Tokura Y 2001 *Science* **291** 2573
[7] Jungwirth T, Qian N and MacDonald A H 2002 *Phys. Rev. Lett.* **88** 207208
[8] Yao Y, Kleinmann L, MacDonald A H, Sinova J, Jungwirth T, Wang D-S, Wang E and Niu Q 2004 *Phys. Rev. Lett.* **92** 037204
[9] Tatara G and Kawamura H 2002 *J. Phys. Soc. Japan* **71** 2613
[10] Campbell I A and Fert A 1982 *Ferromagnetic Materials* vol 3, ed E P Wohlfarth (Amsterdam: North-Holland) p 797
[11] Chen T T and Marsocci V A 1972 *Physica* **59** 498
Chen T T and Marsocci V A 1972 *Solid State Commun.* **10** 783
[12] Bowen M, Friedland K-J, Herfort J, Schönherr H-P and Ploog K H 2005 *Phys. Rev.* B **71** 172401
[13] Friedland K-J, Nötzel R, Schönherr H-P, Riedel A, Kostial H and Ploog K H 2001 *Physica* E **10** 442
[14] Friedland K-J, Muduli P K, Herfort J, Schönherr H-P and Ploog K H 2005 *J. Supercond.* **18** (Published online: 12 July)
[15] Muduli P K, Friedland K-J, Herfort J, Schönherr H-P and Ploog K H 2005 *Phys. Rev.* B **72** 104430
[16] Akgöz Y C and Saunders G A J 1975 *Phys. C: Solid State Phys.* **8** 1387
[17] Schönherr H-P, Nötzel R, Ma W and Ploog K H 2001 *J. Appl. Phys.* **89** 169
[18] Herfort J, Braun W, Trampert A, Schönherr H-P and Ploog K H 2004 *Appl. Surf. Sci.* **237** 181
[19] Herfort J, Schönherr H-P and Ploog K H 2003 *Appl. Phys. Lett.* **83** 3912
[20] Muduli P K, Herfort J, Schönherr H-P and Ploog K H 2005 *J. Cryst. Growth* **285** 514
[21] Muduli P K, Herfort J, Schönherr H-P and Ploog K H 2005 *J. Appl. Phys.* **97** 123904
[22] Herfort J, Schönherr H-P, Friedland K-J and Ploog K H 2004 *J. Vac. Sci. Technol.* B **22** 2073
[23] Jenichen B, Kaganer V M, Herfort J, Satapathy D K, Schönherr H-P, Braun W and Ploog K H 2005 *Phys. Rev.* B **72** 075329
[24] Berger L 1970 *Phys. Rev.* B **2** 4559
[25] Karplus R and Luttinger J 1954 *Phys. Rev.* **95** 1154
[26] Shindou R and Nagaosa N 2001 *Phys. Rev. Lett.* **87** 116801
[27] Fang Z, Nagaosa N, Takahashi K S, Asamitsu A, Mathieu R, Ogasawara T, Yamada H, Kawasaki M, Tokura Y and Terakura K 2003 *Science* **302** 92
[28] Stearns M B 1968 *Phys. Rev.* **168** 588
[29] Szymański M, Jankowski M, Dobrzyński L, Wiśniewski A and Bednarski S 1991 *J. Phys.: Condens. Matter* **3** 4005
[30] Birss R R 1964 *Symmetry and Magnetism* (Amsterdam: North-Holland) chapter 5, section 4
[31] Ye J, Kim Y B, Millis A J, Shraiman B I, Majumdar P and Tesanovic Z 1999 *Phys. Rev. Lett.* **83** 3737
[32] Moss J and Brown P J 1972 *J. Phys. F: Met. Phys.* **2** 358